TEMPERATURE STRATIFICATION IN A ROAD TUNNEL

by

Brahim KALECH[a,b*], Zouhaier MEHREZ[b], Mourad BOUTERRA[b], Afif El CAFSI[b], and Ali BELGHITH[b]

[a] Faculty of Sciences and Technics, Sidi Bouzid, University of Kairouan, Kairouan Tunisia
[b] LETTM, Faculty of Sciences of Tunis, University of Tunis-El Manar, Tunisia, Tunisia

Original scientific paper
DOI: 10.2298/TSCI121226156K

Tests were conducted to study the temperature distribution and stratification of smoke in a tunnel at 1-D propagation phase, the ventilation strategy varies in these trials. Numerical results showed that there are three layers of flow in the different strategies, the smoke layer, intermediate mixture layer, and training fresh air layer. A barrier effect has been shown for the distribution of the temperature of the smoke upstream. The temperature and the velocity of movement of the smoke flow were influenced by the type of ventilation strategy. Stratification of the flow is characterized by a Richardson number. This numerical study requires validation with the work of Hu et al. (ref. 13). However, a good agreement was obtained.

Key words: *tunnel fire, stratification, temperature, fire dynamics simulation*

Introduction

Fire poses a significant threat to life safety in tunnels, there are great dangers to users and equipments. Several catastrophic fires had occurred in tunnels in the past years, and among the known examples in the world were the accidents in Mont-Blanc and Tauern in 1999, Gotthard in 2001, and Dague in 2003.

The smoke temperature and the toxic gases, such as CO, are the most fatal factors in fires.

It is necessary to have a ventilation strategy to control a smoke flow. Same for tunnels that have a ventilation strategy, we conducted research to improve the efficiency of the ventilation system in order to increase the level of security such as the study of Vidmar *et al.* [1].

In any case, the temperature distribution and stratification of the flow are difficult to estimate. Since the stratification of the flow is important for security in a tunnel, it depends on various conditions (the geometry of the tunnel, fire size, *etc.*) and especially the ventilation strategy.

There have been some experiments on the study of the spread of smoke. When a fire broke out in a tunnel, smoke flow development can be summarized in four phases [2]:

– impinging region of rising plume on the ceiling,
– radial spread of smoke under the ceiling after impingement,
– interaction with side walls, and thus the transition region to 1-D spread, and
– 1-D spreading.

* Corresponding author; e-mail: ib.kalech.fst@gmail.com

To ensure adequate protection, the temperature distribution and smoke stratification should be better understood. Such knowledge is important for understanding the evolution of the plume and mainly the smoke flow in tunnels fires at 1-D spreading.

Experimental studies on smoke in a tilted tunnel are performed by the reduced-scale tunnel model [3]. The results show that the smoke spread upwards much faster with the slop gradient increasing, and a thick smoke layer was formed when smoke moved to the upward part of the tunnel and filled it up.

The velocity of ventilation had a great influence on the temperature distribution along the tunnel and the smoke stratification will be distributed when the speed of longitudinal ventilation becomes large.

A series of experiments were carried by Ji *et al.* [4] to investigate the influence of different places cross fire on the maximum temperature in the tunnel ceiling. The results show that the restrictive effect of the side walls of the tunnel causes the temperature increment in the maximum compared with the open space. The maximum temperature of smoke above the fire is almost unchanged and then will increase significantly if the distance between the fire and the side wall decreases to a certain value.

Blanchard *et al.* [5] have experimentally and numerically studied a 1/3 reduced scale tunnel, using a heptane pool fire. They conducted tests for ventilation speeds below and above the critical back-layering velocity to highlight some difficulties to predict the smoke back-layering. Efforts were made to verify the validity of the simulation compared with the experimental databases. In fact, approximately 50-67% of the heat is dissipated through interaction with the wall in the sub-critical and critical regimes.

Two sets of model scale experimental tests were also carried out by Li *et al.* [6]. The heat, longitudinal velocity and the parameters of tunnel geometry are taken into account. The results of analysis and experiments show that the maximum temperature excess gas in the ceiling and the temperature can be divided into two regions. When the dimensionless ventilation velocity is greater than 0.19, the maximum temperature is below the ceiling of the tunnel, it increases linearly with the heat release rate and decreases linearly with the speed of longitudinal ventilation. When the dimensionless velocity ventilation is less than 0.19, the maximum temperature under the ceiling of the gas varies as the third power of two velocity dimensionless heat release, independent of the longitudinal velocity of ventilation.

Yang *et al.* [7] have realized experiments in a horizontal channel to a reduced scale. They studied the behavior of the flow stratification with the rate of aspiration through the opening in the ceiling of channel. The horizontal velocity of the movement, the vertical profile of the temperature and the height of the interface of stratification of the flow dynamics were measured. Based on the Froude number and Richardson number, they proved that the model is divided into three stratification regions.

A study to predict the longitudinal distribution of temperature rise for the smoke layer along a tunnel by Hu *et al.* [8]. The temperature field and smoke layer traveling velocity were measured downstream the fire source. The decay factors for longitudinal smoke layer excess temperature distributions were predicted from the model based on the smoke layer velocities and the dimensions of the vehicular tunnel.

An investigation of previously established correlations between gas temperature distribution and smoke stratification in mines has been carried out for tunnel applications by [9]. The investigated correlations are based on excess gas temperature ratios and Froude number scaling. The temperature data obtained at different locations and different heights have been used for the comparison. A good correspondence between the experimental data and the cor-

relations has been found when the gas temperature data were used. New correlations between the temperature stratification and the Froude number are also explored.

Wang [10] focused on understanding the characteristics of a real-scale tunnel fire in terms of the flame propagation and the toxic gas generation. An extension of the eddy dissipation concept in corporating two chemical reaction steps is integrated into an internationally recognized CFD fire simulation code – fire dynamics simulation, (FDS), 5.5. A full-scale over-ventilated tunnel fire is simulated with the model. The model is then used to investigate the characteristics of a tunnel fire in three aspects of the backlayering length. The effects of blockage in a tunnel on the propagation of smoke and fire are numerically investigated with the model.

This paper presents an investigation of the temperature distribution and stratification of the smoke flow for different ventilation strategies in 1-D spreading.

Numerical model

Numerical-experimental comparison

The use of FDS for calculations of smoke movement in case of fire in tunnel is increasingly popular. This is reflected by a large number of recent journal publications, it is also becoming more and more common practice in search. The computer program can be used to analyze fire related problems, such as temperature, velocity and concentration distribution, FDS has been validated [11, 12] to be capable of simulating the propagation of smoke and transportation of CO species in a channel fire.

The FDS solves numerically a form of the Navier-Stokes equations appropriate for low velocity, thermally-driven flow with an emphasis on smoke and heat transport from fires.

The core algorithm is an explicit predictor-corrector scheme, second order accurate in space and time. Turbulence is treated by means of the Smagorinsky form of large eddy simulation (LES).

The conservation equations for mass, momentum, and energy for a Newtonian fluid are presented here [11]:

– conservation of mass

$$\frac{\partial \rho}{\partial t} + \nabla(\rho u) = \dot{m}_b''' \tag{1}$$

– conservation of momentum

$$\frac{\partial}{\partial t}\rho u + \nabla \rho uu + \nabla p = \rho g + f_b + \nabla \tau \tag{2}$$

– transport of sensible enthalpy

$$\frac{\partial(\rho h_s)}{\partial t} + \nabla \rho h_s u - \frac{Dp}{Dt} = \dot{q}''' + \dot{q}_b''' - \nabla \dot{q}''' + \varepsilon \tag{3}$$

– equation of state for a perfect gas:

$$p = \frac{\rho \mathrm{R} T}{\bar{W}} \tag{4}$$

The application of LES technique to fire is aimed at extracting greater temporal and spatial fidelity from simulation of fire. This model explicitly calculates the turbulent large scales and models the effects of smaller ones using subgrid closure rules. The approach based on LES has a particular advantage over the Reynolds-averaging procedures in that only the effects of small-scale turbulence motion have to be modeled. The FDS code adopts the *low Mach number* combustion equations that describe the low speed motion of a gas driven by chemical heat release and buoyancy forces.

In predicting smoke movement by LES, two points should be considered [11, 12]:

– fine enough grids, and
– a suitable sub-grid model (SGM) on small eddies.

The LES SGM commonly used in LES was developed originally by Smagorinsky. A refined filtered dynamics SGM was applied in the FDS model to account for the sub-grid scale motion of viscosity, thermal conductivity and material diffusivity [12]. The dynamic viscosity defined in FDS is:

$$\mu_{\mathrm{LES}} = \rho\,(Cs\Delta)^2\left[2\overline{S_{ij}}\,\overline{S_{ij}} - \frac{2}{3}(\nabla\vec{\mathrm{u}})^2\right]^{1/2} \tag{5}$$

where Cs is the constant of Smagorinsky, $\Delta = (\delta x\,\delta y\,\delta z)^{1/3}$ and

$$|S| = 2\left(\frac{\partial u}{\partial x}\right)^2 + 2\left(\frac{\partial v}{\partial y}\right)^2 + 2\left(\frac{\partial w}{\partial z}\right)^2 + \left(\frac{\partial u}{\partial x} + \frac{\partial v}{\partial y}\right)^2 +$$

$$+\left(\frac{\partial u}{\partial z} + \frac{\partial w}{\partial x}\right)^2 + \left(\frac{\partial v}{\partial z} + \frac{\partial w}{\partial y}\right)^2 - \frac{2}{3}(\nabla\vec{\mathrm{u}})^2 \tag{6}$$

The term $|S|$ consists of second-order spatial differences averaged at the grid centre. The thermal conductivity k_{LES} and material diffusivity D_{LES} of the fluid are related to the viscosity μ_{LES} in terms of the Prandtl and Schmidt numbers by:

$$k_{\mathrm{LES}} = \frac{C_p\mu_{\mathrm{LES}}}{\mathrm{Pr}}, \qquad (\rho D)_{l,\mathrm{LES}} = \frac{\mu_{\mathrm{LES}}}{\mathrm{Sc}} \tag{7}$$

Both Prandtl and Schmidt numbers are assumed to be constant. The specific heat, C_p, is taken to be that of the dominant species of the mixture [11, 12]. The constants Cs, Pr, and Sc are equal to 0.2, 0.2, and 0.5, respectively.

The Courant-Friedrichs-Lewy (CFL) was used in FDS [12] for justifying convergence. This criterion is more important for large-scale calculations where convective transport dominates the diffusive one. The estimated velocities are tested at each time step to ensure that the CFL condition is satisfied [12]:

$$\max\left(\frac{|u_{ijk}|}{\delta x}, \frac{|v_{ijk}|}{\delta y}, \frac{|w_{ijk}|}{\delta z}\right) < 1$$

The time step is eventually changed to a quasi-steady value when the fire burns steadily. The results from a numerical analysis are sensitive to the grid size used. In this study, we are sure that the CFL condition is satisfied for the first time step in order to obtain a good convergence.

For the realization of their numerical experiments, the authors used the geometry shown in figs. 1 and 2 [13]. Initially, we follow the same pattern with the same boundary conditions for the comparison of results.

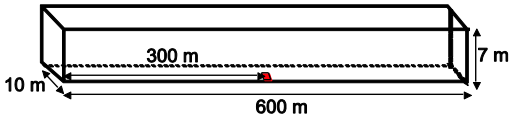

Figure 1. Geometrical configuration adopted for comparison

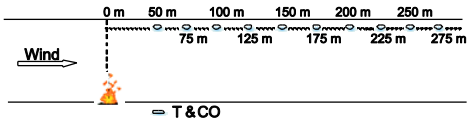

Figure 2. The positions of thermocouples for measuring the temperature and CO concentration [13]

Fire is simulated by a source placed at the center of the tunnel. Fire power is determined by the command heat release rate per unit area (HRRPUA) provided in FDS. The combustion model used is the mixture fraction *Mixture Fraction* implemented in the model of turbulent LES.

The type of reaction is crude oil, CRUDE OIL, according to the data of the reactions of FDS code. This reaction is specific for the production of smoke and the dispersion of CO from the fire source. The fraction of the fuel converted to CO, y_{CO}, is related to the fraction of the efficiency of the soot, y_s.The y_s value was set at 0.1 according to the CRUDE OIL [14].

The inner material is defined as concrete, CONCRETE, based on data provided by FDS. The dimensions of the source of fire is 2 m^2 (2 m × 1 m), 4 m^2 (2 m × 2 m), and 6 m^2 (3 m × 2 m) corresponds for the power of such a fire is 4, 10, and 20 MW, heat output of a burning a car, a bus and a truck. In this study, the HRRPUA is steady for all simulations.

Both ends of the tunnel are naturally open, without initial speed. The velocity of longitudinal ventilation of fresh air flow along the tunnel is set-up by the command MISC provided by FDS. With this method, the velocity of longitudinal ventilation of fresh air flow is uniform in tunnel.

The mesh is linear along the tunnel, the fire zone is 20 m and Δx = 0.2 m. The Δx = 0.5 m on both sides of the fire area. The mesh is uniform according to y and z, $\Delta y = \Delta z$ = 0.2 m.

In FDS, a measure defined as the non-dimensional expression of $D^*/\Delta x$ is introduced [12] to test how well the fire is resolved by the grid system. Here D^* is the characteristic fire diameter and Δx is the nominal grid cell size:

$$D^* = \sqrt[5]{\left(\frac{Q}{\rho_a C_p T_a \sqrt{g}}\right)^2}$$

When the numerical grid is coarse, the stoichiometric surface $Z = Z_f$ underestimates the observed flame height. An empirical relation has been found to estimate the flame height:

$$\frac{Z_{f,\mathrm{eff}}}{Z_f} = \min\left(1, C_f \frac{D^*}{\Delta x}\right)$$

For the grid system used in this paper, the value of $C_f D^*/\Delta x$ is 6.7, 9.66, and 13.33 for the 4, 10, and 20 MW fire, respectively, all being much larger than 1. This indicates that the grid system is fine enough to resolve the fire with no approximation implemented.

Normalized by the value at the +50 m position, the comparison of longitudinal distributions of temperature and CO concentration computed by FDS for both works for a same scenario are shown in figs. 3 and 4. The size of the fire which is tested equal to 4 MW with longitudinal ventilation velocity of 0.5 m/s.

The recorded values of our simulation for the longitudinal distribution of CO have an error rate of from 2-5%. For the error rate in fig. 4, the results showed that no more than 2%. The consistency of our results is shown in the temperature distribution. The numerical results are in good agreement with the theoretical model and as validated with them results of Hu *et al.* [13].

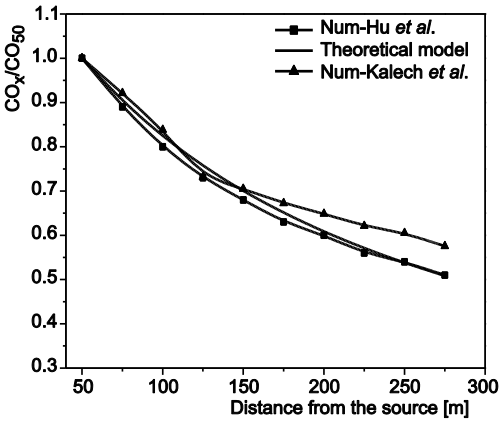

Figure 3. The longitudinal profile of CO concentration (Q = 4 MW, U = 0.5 m/s)

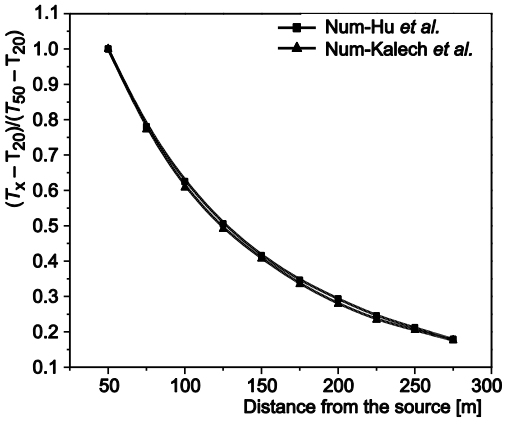

Figure 4. The longitudinal profile of temperature (Q = 4 MW, U = 0.5 m/s)

Configuration for simulation

After having adjusted the parameters of study, the constants of turbulence model, constants of combustion model, and especially the mesh, we propose the geometric configuration adopt for simulation as shown in fig. 5 with its geometrical dimensions, such as the length L = 300 m, the width W = 10 m, and the height h = 5 m. For all simulations, the heat release rate was used Q = 10 MW to represent the fire.

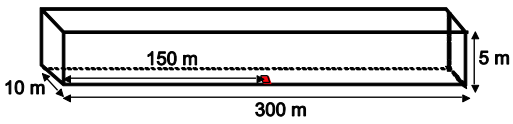

Figure 5. Geometrical configuration adopted for simulation

The source of fire keeps the same characteristics as that used for comparison. The openings in the ceiling have square cross-sections (S) of the width d = 2 m and the height of false ceiling thickness H' = 0.2 m for the four cases (fig. 6).

An important concept in the convective motions of hot gas is that the movement is always in the direction of higher pressures to lower pressures. To do this, we chose to base on the natural ventilation strategy in different geometric configurations available at figs. 6(a)-(c).

Figure 6(a) characterizes chimney effect with a height of 2 m, which is due to the pressure difference between the air inside and the air outside of the tunnel. This factor has a significant influence especially at times when the differences between indoor and outdoor temperatures are high. Figures 6(b) and (c) show the second and third cases. The exhaust duct is a height equal to 1 m above the ceiling. The second shows an aspiration in the exhaust duct

above openings there is to create a depression area. Figures 6(d) and (e) show the effect of the longitudinal velocity of ventilation and aspiration through the exhaust duct, respectively, for the longitudinal ventilation strategy and transversal ventilation strategy.

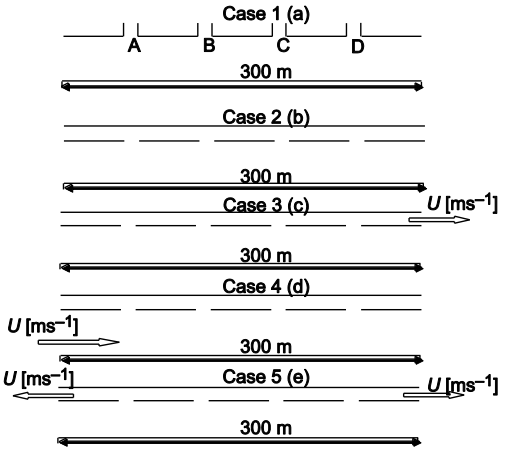

Figure 6. Geometrical configuration for all cases

Results and discussion

The simulation results of temperature distribution are shown in figs. 7 and 8, the velocity profile in figs. 8-10, and the vertical profile of Richardson number in figs. 11-13. The results of the analysis are shown with different scales in tunnel (x) and height (z) directions. The results are discussed.

The hot combustion products are compared to the ambient air and are therefore subject to the forces of gravity upward. They form a plume rising above the origin of the fire and they result from the ambient air. The suction speed does not affect the slope of the plume and the flow is symmetrical.

The smoke is developed on both sides of the fire before reaching the ceiling, fig. 7(a). Without aspiration, fig. 7(b), the tunnel is almost filled of smoke up 80% to tunnel height (h). The maximum temperature occurs at a distance below the ceiling, about 50% of h and between the openings. Between the two openings B and C, the temperature recorded is 800 °C. Between the openings (A-B, and C-D), the temperature is between 60 and 110 °C. At the fire source, the value of the recorded temperature is of the order of 820 °C. In the lower half of the tunnel, as the vertical profile, the temperature is rapidly degraded, and the recorded values are from 20-110 °C. From both sides of the openings A and D, the temperature is 20-70 °C. The temperature distribution is similar in the first two cases.

For case 3, with a speed of aspiration to the right, fig. 7(c), the smoke flows similarly than cases 1 and 2 for the temperature field in advance of the tunnel. At the upstream side of the tunnel, the temperature values are lower than those without aspiration.

By increasing the intensity of the suction velocity, fig. 7(d), the layer of smoke flows just below the ceiling and the tunnel is filled with smoke at 40% of h. The temperatures between the openings A and D, is 60-400 °C. To the left of the opening A, the temperature reaches 50 °C maximum. On the other hand, the smoke does not reach the right side of the tunnel and the temperature equal to that of ambient, 20 °C.

The longitudinal velocity of ventilation acts as a barrier against the flow of the fumes upstream of the tunnel, fig. 8(a).

When the air velocity is less than critical velocity of ventilation, we observed the phenomenon of back-layering. The critical velocity of ventilation is on the order of 2.2 m/s for a 10 MW fire power. At the critical velocity of ventilation, fig. 8(b), practically the all quantity of smoke is pushed in the downstream side. With a back-layering of the smoke below the ceiling which is 20 m in length and 20% of h.

The temperature varies between 110 °C and 450 °C, it is higher and is distributed in the upper half of the tunnel. It degrades in relation to the length of the tunnel. The instability of the flow affects the temperature distribution.

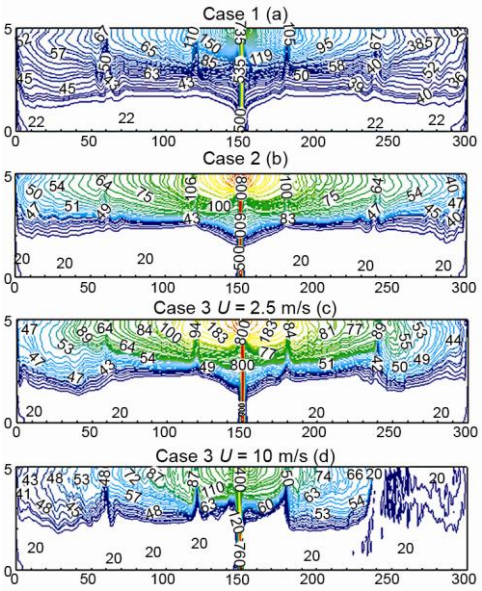

Figure 7. Temperature fields [°C]

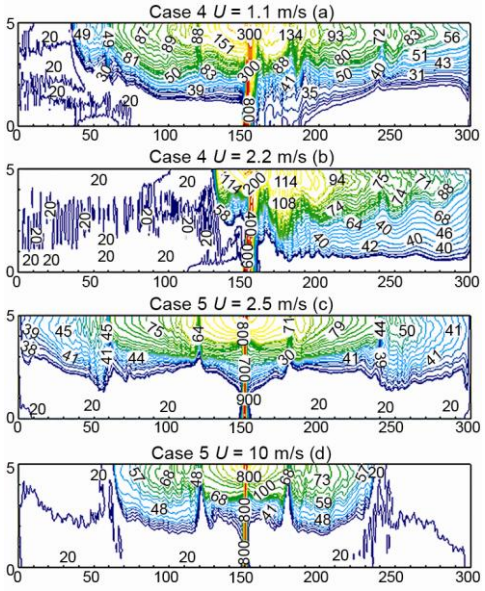

Figure 8. Temperature fields [°C]

Physically, when a velocity is applied to the plume, and this causes the inclination to increase the amount of entrained air, the burning rate. and heat flux radiated is increased. Faced with this situation, the flame behaves like a pseudo-obstacle. Flame tilts under the effect of the dynamic pressure exerted by the transverse component of the velocity and its envelope undergoes a structural change. At the upstream or downstream, there is the presence of an overpressure zone.

For the 5th case, figs. 8(c) and (d), the flow is symmetrical with respect to the source of fire. The plume develops in a symmetrical manner on either side of the source. The highest temperature recorded is below the ceiling, it is between the openings A and D. The recorded values are between 60 °C and 800 °C.

Note that the strategy of the longitudinal ventilation is important in regard to the direction in which the fire propagation and stratification of smoke. Large air velocities tend to limit the phenomenon of back-layering upwind of fire. The layer of smoke was observed over a height between 40% and 60% of *h* from the ceiling. The transversal ventilation strategy is intended to maintain the stratification layer under the ceiling. Smoke is vented from the exhaust duct above the tunnel.

The profiles of the flow velocity of smoke based on the height are shown in fig. 9 in different sections of the tunnel to the 2nd and 3rd cases.

The upstream side of the tunnel, the smoke flow with a speed U = 1.5 m/s. While approaching the fire source, the speed of the smoke layer reached 2 m/s. It was found that the suction velocity applied does not affect the speed of the flow of smoke. Also, an amount of entrained air was observed, it flows to 1 m/s at the inlet section of the tunnel, and increases in approaching the source up reached 1.5 m/s.

The downstream side of the tunnel, the velocity of the smoke layer reached 2.5 m/s and an air speed driven 1.5-2 m/s to the section x = 270 m. By increasing the intensity of the suction velocity, the profile becomes flat at x = 270 m for a speed of 10 m/s.

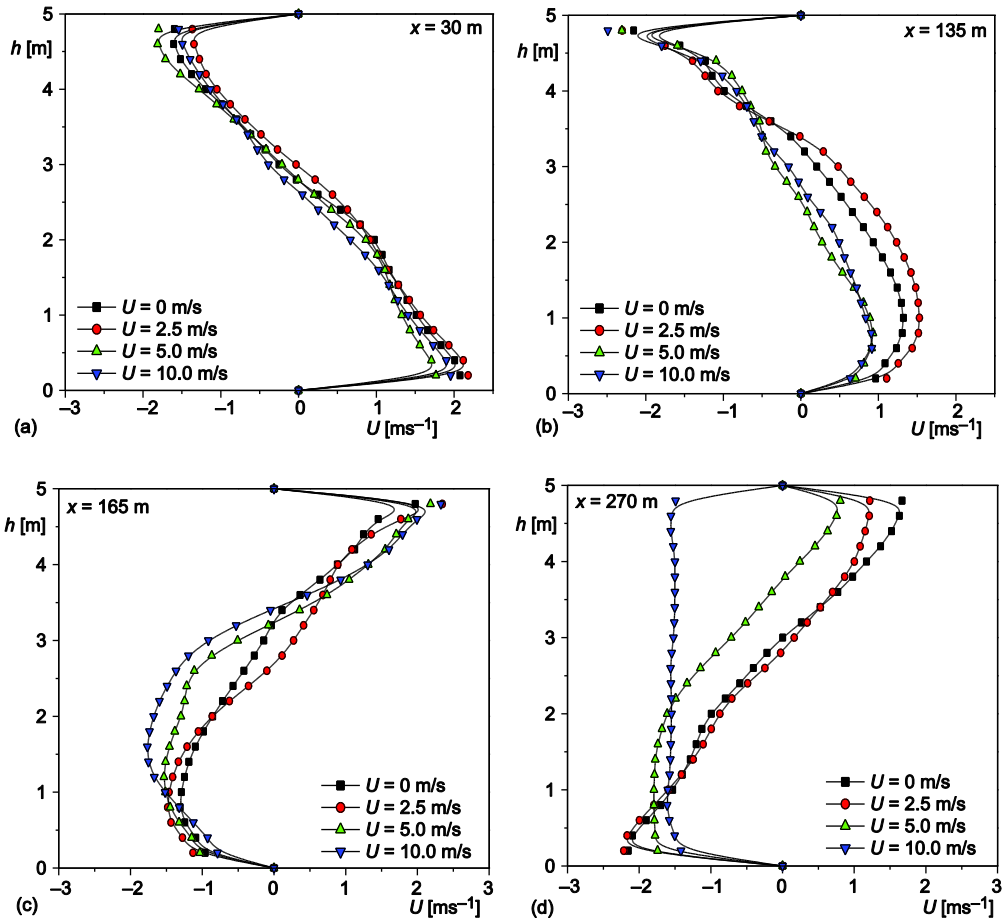

Figure 9. Velocity profile, cases 2 and 3

Generally in these natural conditions, velocity profile admits an inflection point. It means that the flow is controlled by a layer of smoke flowing below the ceiling. It confirms, also, the existence of a layer laminated below.

In the presence of longitudinal ventilation, the flow velocity is changing rapidly increasing the intensity of the fan speed, fig. 10. The curvature takes the form continues at the upstream section of the tunnel, x = 30 m. In section 135 m, while approaching the source, the profiles admit inflection points. The velocity of the smoke flow (U) varies between 1.5 m/s and 2.5 m/s. The flow takes the form of the continuous profile for the case of longitudinal velocity equal to 2.2 m/s.

Downstream of the source, the velocity of the smoke flow is from 1-4 m/s, respectively, for the velocity of ventilation (V) between 0 m/s and 2.2 m/s. The profiles are almost flat, which explains the homogenization of the flow.

By increasing the intensity of the longitudinal velocity, the sections 165 m and 270 m, the profiles tend to be flat. The velocity of smoke flow increases.

The distribution of buoyancy flow between the upstream and downstream of the source in the presence of longitudinal ventilation has a great influence on the speed of the

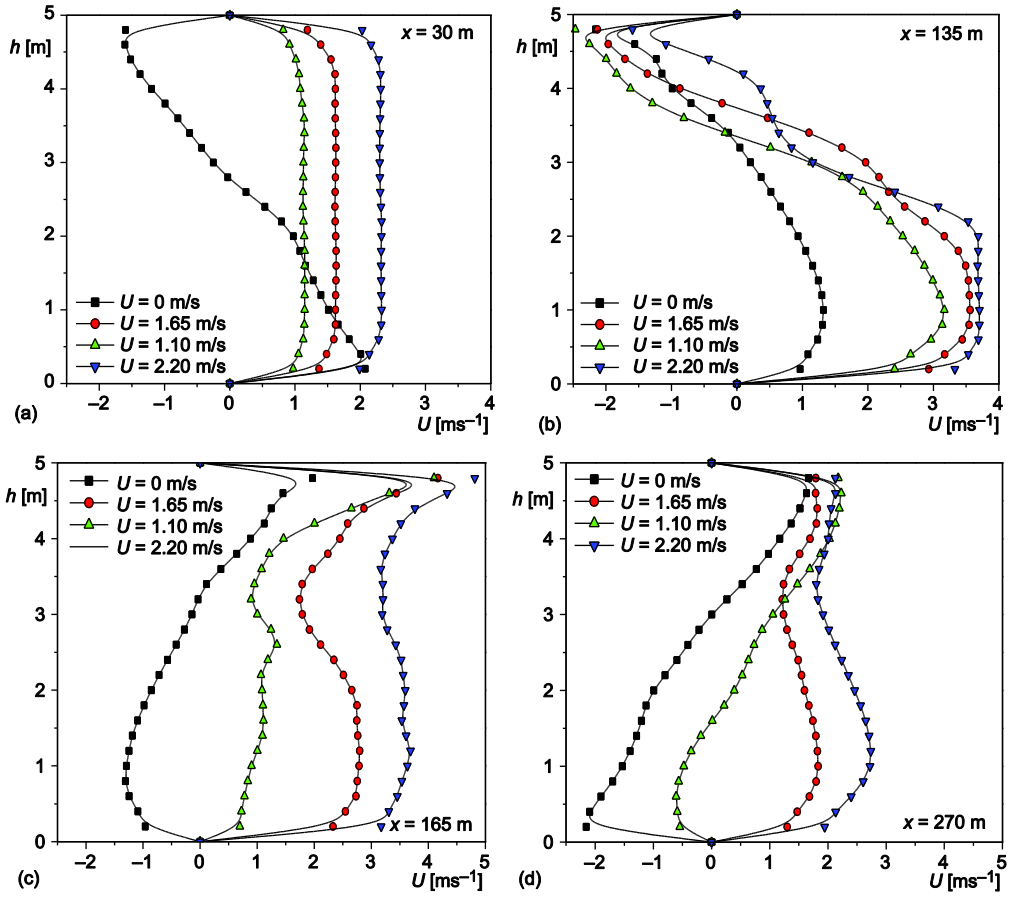

Figure 10. Velocity profile, case 4

smoke flow under the ceiling. A mixture layer is produced in the flow. This is the case for the backlayering in confirmation with the flow of ventilation air. Analysis of the mechanism showing the negative effect of the speed of the longitudinal ventilation on stratification.

Figure 11 shows the vertical profiles of the flow velocity for cross ventilation strategy. The results show that the flow is symmetric with respect to the source of fire. Upstream and downstream sections, x = 30 m and 270 m, the profiles are flat view the large size of the suction velocity, U = 5 m/s and 10 m/s. The openings (A and D) aspire in ambient air with the smoke.

The upstream and downstream sections of source, x = 135 m and 165 m, the flow velocity between 1.5 m/s and 2.5 m/s and the profiles allow an inflection point. This confirms the existence of a layer of smoke which drives the flow. Stratification is likely to continue.

Fields horizontal temperature also provides information on the thermal homogenization of the various layers of the smoke. To better understand this phenomenon, we propose to study the profile of the Richardson number. Richardson number gives a physical point of view of the phenomenon, $\mathrm{Ri} = g\beta\Delta TL_c/U^2$. To locate the different symptomatically areas of the overall flow, we propose to calculate the local Richardson number in each measurement point, figs. 12, 13, and 14.

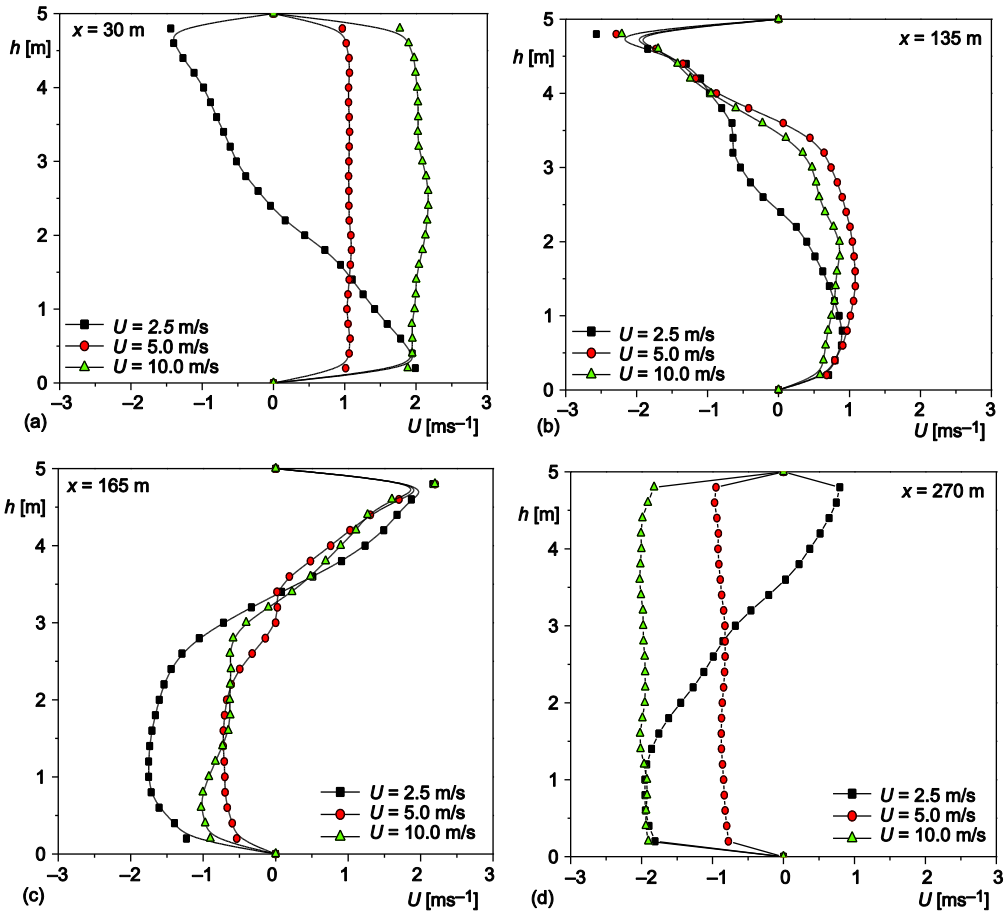

Figure 11. Velocity profile, case 5

By definition, the value of the Richardson number and profile curvature are indicative of the stability of the stratification of the flow. In addition, speed affects the Richardson number. When the speed is very low, high shear, the Richardson number tends to a large value. The variations in the thickness of the mixing layer seem to depend mainly on the movement kinematics related to the vortices (shear).

When a layer of smoke flows freely from the ceiling of the tunnel, a call for fresh air is generated, as shown in the velocity profile, rushing at ground level. Throughout the path of the layer, the two flows are opposed in an area, generally called interface, which shear phenomena cause mixing. The flow seems to cut in layers separated by an area of high Richardson number that acts as a *barrier*. This effect is well illustrated in the vertical profiles (figs. 12, 13, and 14). The peaks are the number one for all cases.

At the upstream section of the tunnel, x = 30 m, the Richardson number is around 3 for all cases of simulation. This observation is valid for the section downstream of the tunnel, x = 270 m. Note that the flow is stratified. For the 3rd case, U = 10 m/s, the smoke are extracted from the opening D and they do not arrive at the downstream side of the tunnel.

The mixing zone is located between the elevations z1 and z2 where the product of destratification of the smoke layer. It is difficult to distinguish this area. This turbulence area

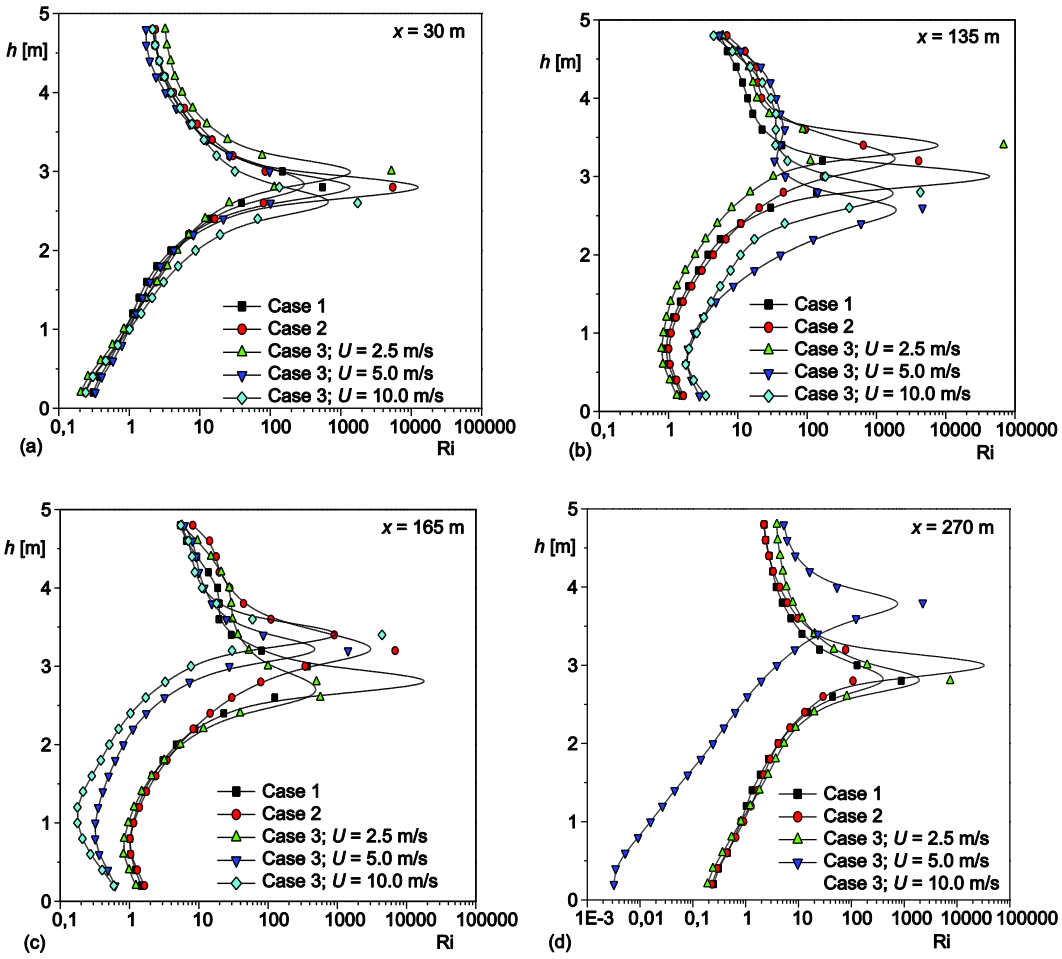

Figure 12. The vertical profile of Richardson number

is subject to the combined actions of the shear between the two flows and the forces of gravity acting on the smoke layer. The mixing zone can then be carried out to a depth of thickness between 5% and 20% of the height *h*. The layer of smoke under the ceiling has a thickness between 10% and 25% of the height *h*. The entrained air is carried out over a height between 25% and 50% of *h* between the floor and the ceiling.

Figure 13 shows the vertical profiles of the Richardson number to different sections of the tunnel for the longitudinal ventilation strategy. To the different sections, in the absence of the longitudinal velocity, the flow is divided into three zones: a smoke layer to below the ceiling, an intermediate layer characterized by a peak number of Richardson, and on an entrained air.

The evolution of the longitudinal velocity affects on the thickness of the layer of smoke. The upstream section of the source, x = 135 m, the layer of smoke flow is delaminated. The layer of the smoke is of a height between 15% and 20% of *h* from the ceiling.

Downstream of the source and in the presence of a longitudinal velocity, x = 165 m, recall that the velocity profile is flat shape and well for the Richardson profile. This situation

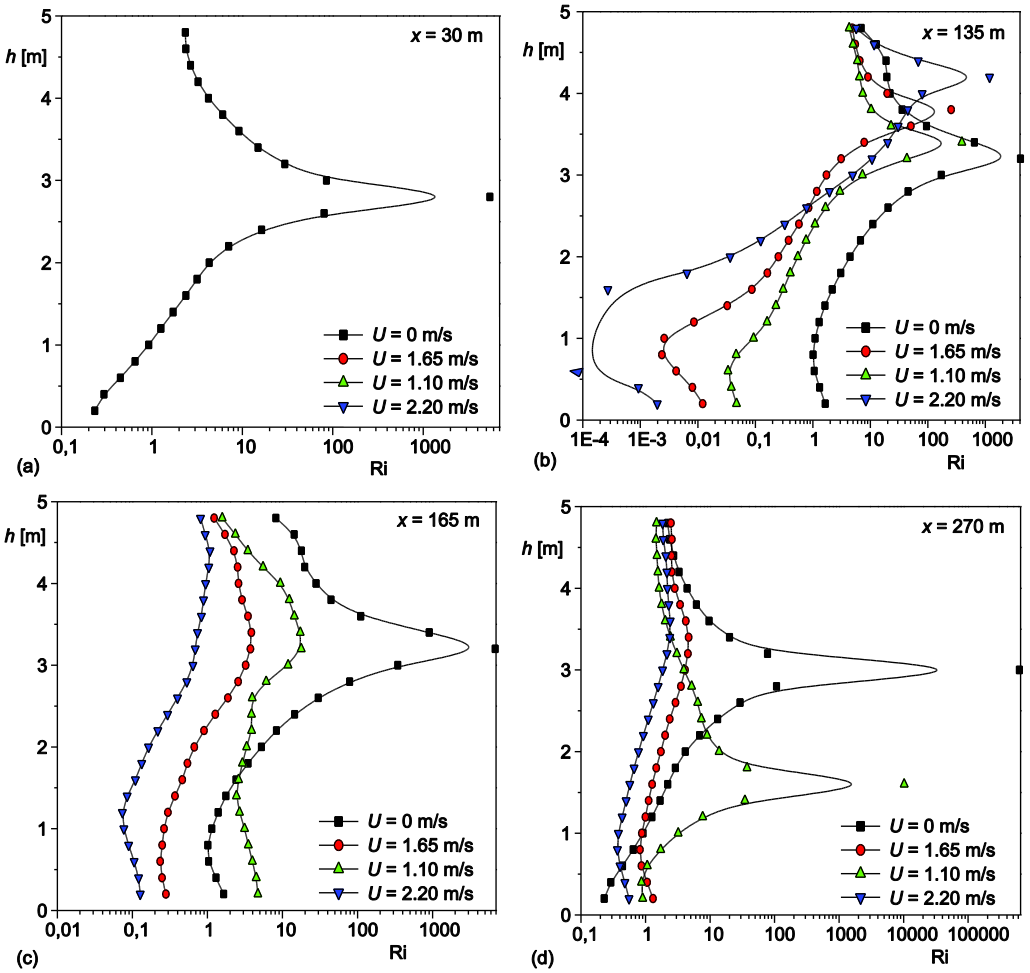

Figure 13. The vertical profile of Richardson number, case 4

reflects the strong local destratification. Note also that the vertical temperature gradient is generally low. The smokes occupy the entire cross section of the tunnel.

To the downstream section of the tunnel, x = 270 m, the layer of the smoke is of a height varying between 5% and 20% of h from the ceiling. It decreases with increasing of the longitudinal velocity. the smoke entirely fill the downstream side of the tunnel for a velocity of ventilation equal to 2.2 m/s. Note that the flow is not stable for all cases. Richardson profiles are flat in shape and Richardson number is around 10.

In case of transversal ventilation, the flow is symmetrical with respect to the fire from the fields of temperature and speed profiles. Figure 14 shows the profiles of the Richardson number, it confirms the general flow stability and the existence of three distinct zones. Fumes layer decreases with increasing speed of aspiration. The thickness of the smoke layer is 20% of h. It decreases with increasing the velocity of aspiration.

The upstream and downstream sections of the fire, x = 135 m and 165 m, the Richardson number is around 9 and laminating the layer of smoke is disrupted. In practice, all the amount of pollutant extracted through the openings.

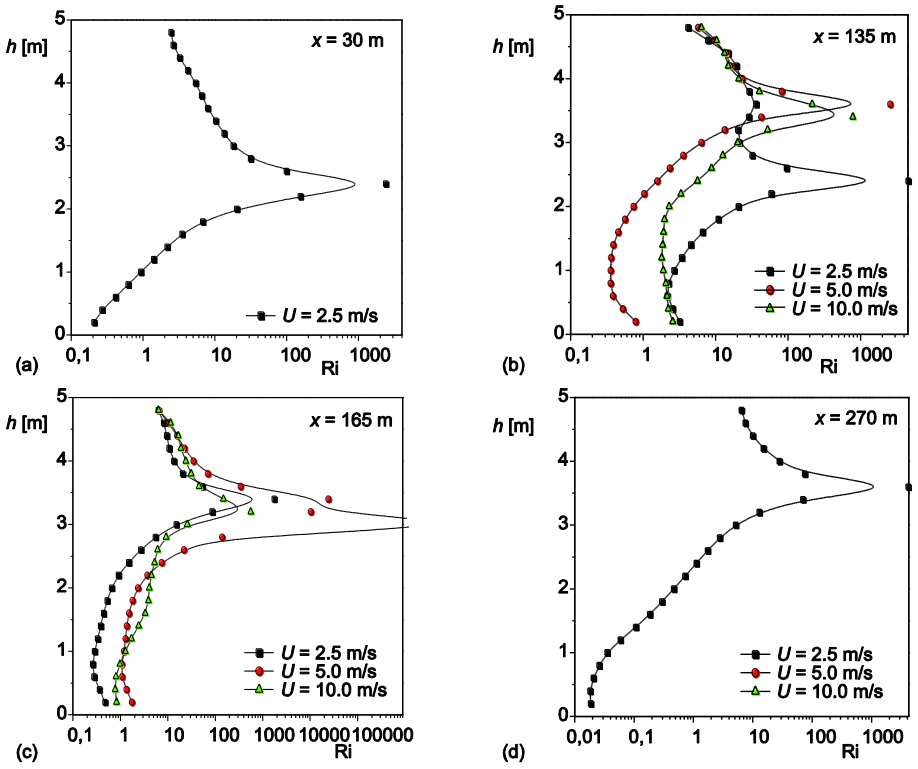

Figure 14. The vertical profile of Richardson number, case 5

Conclusions

Full-scale tests with CFD simulations by FDS version 5.5 were performed to study the smoke temperature distribution in a tunnel fire. The CFD simulations were verified first by the measured data. The results of this study have shown that the model is promising in qualitatively examining the propagation of smoke and the temperature stratification.

The highest temperature is below the ceiling and it degrades according to the length of the tunnel. The maximum velocity and the maximum temperature occur at a distance below the ceiling of about 20% of *h*. The profile of Richardson number confirms the existence of three flow zones.

Basically phenomenological, smoke stratification is maintained below the ceiling of tunnel. The flow of the smoke layer is stable for natural ventilation strategy.

The longitudinal speed of the ventilation favors the homogenization of the flow. The profiles of the Richardson number tend to be flat by increasing the intensity of the velocity. This means that the flow is totally unstable.

Based on the criterion of flow stratification, using the configuration of the case three because it can be adapted to different types of tunnels, the natural ventilation strategy has an advantage relative to the longitudinal strategy.

In the transversal ventilation strategy, the smoke layer is maintained below the ceiling, between the two openings A and D, at height 20% of *h* from the ceiling. The smoke flow is perfectly stratified.

Nomenclature

Cf – empirical constant
C_p – specific heat, [kJkg^{-1}K^{-1}]
Cs – Smagorinsky constant (LES)
d – opening length, [m]
D_{LES} – material diffusivity
f_b – external forces, [Jm^{-3}]
g – acceleration of gravity, [ms^{-2}]
H – exhaust duct height, [m]
H' – false celing height, [m]
h – tunnel height, [m]
k_{LES} – thermal conductivity, [Wm^{-1}K^{-1}]
L – tunnel length, [m]
Pr – Prandtl number, [–]
Q – heat release rate of the fire, [kW]
$\dot{q}'''$ – conductive and radiative heat fluxes, [Wm^{-3}]
Ri – Richardson number, [–]
S – opening cross-section area, [m^2]
Sc – Schmidt number, [–]
T – temperature, [°C]
U – velocity, [ms^{-1}]
V – velocity of ventilation, [ms^{-1}]
W – tunnel width, [m]
Δx, Δy, Δz – the dimensions of the smallest grid cell, [m]

Greek symbols

β – coefficient of thermal expansion, [K^{-1}]
μ_{LES} – viscosity
ρ – density, [kgm^{-1}]
τ_{ij} – stress tensor, [Wm^{-3}]

References

[1] Vidmar, P., *et al*., Upgrade of a Transverse Ventilation System in a Bi-Directional Tunnel, *Thermal Science, 16* (2012), 3, pp. 1067-1080
[2] Kunsch, J. P., Critical Velocity and Range of a Fire-Gas Plume in a Ventilated Tunnel, *Atmospheric Environment,* (1999), 33, pp. 13-24
[3] Li, J., *et al.,* Experimental Study of Smoke Spread in Titled Urban Traffic Tunnels Fires, *Procedia Engineering, 45* (2012), Oct., pp. 690-694
[4] Ji, J., *et al*., Experimental Investigation on Influence of Different Transverse Fire Locations on Maximum Smoke Temperature under the Tunnel Ceiling, *International Journal of Heat and Mass Transfer*, *55* (2012), 17-18, pp. 4817-4826
[5] Blanchard, E., *et al*., Experimental and Numerical Study of Fire in a Midscale Test Tunnel, *Fire Safety Journal, 47* (2012), Jan., pp. 18-31
[6] Li, Y.-Z., *et al.,* The Maximum Temperature of Buoyancy-Driven Smoke Flow beneath the Ceiling in Tunnel Fires, *Fire Safety Journal, 46* (2011), 4, pp. 204-210
[7] Yang, D., *et al.*, Experimental Study on Buoyant Flow Stratification Induced by a Fire in a Horizontal Channel, *Applied Thermal Engineering, 30* (2010), 8-9, pp. 872-878
[8] Hu, L. H., *et al*., Decay of Buoyant Smoke Layer Temperature along the Longitudinal Direction in Tunnel Fires, *Journal of Applied Fire Science, 13* (2004), 1, pp. 53-77
[9] Haukur Ingason, H. Y., Temperature Stratification in Tunnels, *Fire Safety Journal, 48* (2012), Feb., pp. 30-37
[10] Wang, H. Y., Numerical and Theoretical Evaluations of the Propagation of Smoke and Fire in a Full--Scale Tunnel, *Fire Safety Journal, 49* (2012), Apr., pp. 10-21
[11] McGrattan, K., *et al.,* Fire Dynamics Simulator (Version 5.5) Technical Reference Guide, *NIST Special Publication, 3* (2010), Oct., pp. 1-298
[12] McGrattan, K., *et al.,* Fire Dynamics Simulator (Version 5.5) User's Guide, *NIST Special Publication, User Guide* (2010), Oct., pp. 1-222
[13] Hu, L. H., *et al*., Longitudinal Distributions of CO Concentration and Difference with Temperature Field in a Tunnel Fire Smoke Flow, *International Journal of Heat and Mass Transfer, 53* (2010), 13-14, pp. 2844-2855
[14] Hu, L. H., *et al.,* Modeling Fire-Induced Smoke Spread and Carbon Monoxide Transportation in a Long Channel: Fire Dynamics Simulator Comparisons with Measured Data, *J. Hazard. Mater, 140* (2007), 1-2, pp. 293-298

Paper submitted: December 26, 2012
Paper revised: February 10, 2013
Paper accepted: May 12, 2013